11-1990

Adsorption to dipalmitoylphosphatidylcholine membranes in gel and fluid state: pentachlorophenolate, dipicrylamine, and tetraphenylborate

Pavel Smejtek
Portland State University

S. R. Wang

Citation Details
Smejtek, Pavel, and S. R. Wang. "Adsorption to dipalmitoylphosphatidylcholine membranes in gel and fluid state: pentachlorophenolate, dipicrylamine, and tetraphenylborate." Biophysical journal 58.5 (1990): 1285-1294.

Adsorption to dipalmitoylphosphatidylcholine membranes in gel and fluid state: pentachlorophenolate, dipicrylamine, and tetraphenylborate

Pavel Smejtek and Shanru Wang
Department of Physics and Environmental Sciences and Resources Doctoral Program, Portland State University, Portland, Oregon 97207-0715 USA

ABSTRACT We measured the dependence of electrophoretic mobility of dipalmitoylphosphatidylcholine (DPPC) vesicles on the aqueous concentration of negatively charged ions of pentachlorophenol (PCP), dipicrylamine (DPA), and tetraphenylborate (TPhB). The objective was to determine how the physical state of hydrocarbon chains of lipids affects adsorption of lipophilic ions. The studies were done at 25 and 42°C to determine adsorption properties of DPPC membrane in the gel and fluid state, respectively. From the analysis of ζ-potential isotherms in terms of Langmuir-Stern-Grahame model we obtained the association constant, K, the area of the adsorption site, P_s, and the linear partition coefficient, β. Results: K, ($\times 10^4 M^{-1}$): K(gel): PCP (0.49 ± 0.28), DPA (25 ± 10), TPhB (31 ± 10); K(fluid): PCP (4.5 ± 0.9), DPA (74 ± 21), TPhB (59 ± 14); P_s, (nm^2): P_s(gel): PCP (5.4 ± 2.3), DPA (5.9 ± 2), TPhB (5.0 ± 1.7); P_s(fluid): PCP (4.5 ± 0.4), DPA (5.2 ± 0.4), TPhB (4.1 ± 0.2); β, ($\times 10^{-5}$ m): β(gel): PCP (0.15 ± 0.09), DPA (7.1 ± 0.3), TPhB (10 ± 7); β(fluid): PCP (1.7 ± 0.3), DPA (24 ± 7), TPhB (24 ± 6). It was interesting to find that the adsorption site area for PCP, DPA, and TPhB were very similar for both the gel and fluid membranes; also, the areas were independent of the size and molecular structure of the adsorbing species. Using a simple discrete charge model the adsorption site areas for all species were consistent with a dielectric constant of 8–10 and with an ion adsorption depth of 0.4–0.6 nm below the water/dielectric interface. The $\Delta\Delta G^0 = \Delta G^0$(gel) $- \Delta G^0$(fluid) was found to be about twice as large for PCP than for DPA and TPhB. This indicates that PCP will be significantly more adsorbed in the fluid and disordered regions of biomembranes, whereas the distribution of DPA and TPhB is expected to be relatively more even.

INTRODUCTION

To describe the interaction of xenobiotics with biological membranes, one needs to first understand their interaction with lipid bilayers and develop insight into the relationships between the molecular structure of both the xenobiotic molecule and the lipid bilayer matrix.

The present study is concerned with pentachlorophenol (PCP), a highly toxic environmental pollutant, and addresses two questions: (*a*) how does the physical state of lipids in target membranes affect the adsorption of negatively charged PCP^-, and (*b*) how do the adsorption characteristics of PCP^- compare with those of well-known lipophilic ions used as membrane probes: tetraphenylborate ($TPhB^-$) and dipicrylamine (DPA^-). The answers are expected to guide the development of molecular mechanisms of chlorophenol's toxicity to membranes along with useful information for the biophysics and biochemistry of lipid membranes.

Toxicity of PCP has been associated with its presence in biomembranes and uncoupling of ATP synthesis from the electron transport chain (1, 2). Small amphipathic molecules such as PCP are expected to intercalate into the lipid matrix of biomembranes and perturb their structure as Maher and Singer (3) showed for 2,4-dinitrophenol. Our earlier work (4) has shown that PCP decreases the gel-to-fluid phase transition temperature of phosphatidylcholine (dimyristoylphosphatidylcholine [DMPC] and dipalmitoylphosphatidylcholine [DPPC]) membranes. PCP alters the physical properties of membranes and was found to induce electrical conductivity in lipid bilayers (5, 6). Toxicity in algae (7) was related to induced membrane conductivity by the transmembrane transfer of protons (5–7). Solvatochromic shifts of absorption spectra of PCP^- and changes in the pK_a of PCP adsorbed to phosphatidylcholine (PC) membranes suggested that the adsorption sites of PCP^- are located at some depth below the membrane surface (8).

In this work we have compared the interaction of PCP^- and two benchmark lipophilic ions $TPhB^-$ and DPA^- with DPPC membranes. These lipophilic ions have been extensively used in membrane studies (9–12). It is well known that these ions, similar to PCP^-, are adsorbed at some depth within the membrane. Adsorption of positively and negatively charged lipophilic ions has been successfully treated by the dipolar model of lipid bilayer membranes developed by Flewelling and Hubbell (13). Also, the interactions of small molecules with membranes have been recently reviewed in reference 14.

Address correspondence to Pavel Smejtek.

We have selected DPPC in studying the effect of conformational order of hydrocarbon chains of lipids on the adsorption of lipophilic ions in membranes. The major reason for selecting DPPC membranes is that they are the best understood model for phospholipid membranes (15). Their gel-to-fluid phase transition temperature, ~41°C (16), is conveniently positioned for experimental studies of both the gel and fluid states of membranes. In the gel L_β state the hydrocarbon chains are fully extended and tightly packed, resulting in 0.46 nm^2 (15) per lipid and a membrane thickness of 5.6 nm (15, 17). In the fluid L_α phase the chains are disordered resulting in a thinner membrane, 4.4 nm (17) with a significantly larger membrane surface area per lipid, 0.71 nm^2 (18).

While taking into consideration the scatter of thermodynamic data pertinent to adsorption of lipophilic ions of our interest (e.g., Table 2 in reference 19), we concluded to use one method of determination and one set of experimental conditions to obtain meaningful results. The adsorption characteristics as reported here were obtained from the dependence of electrophoretic mobility of DPPC vesicles on the aqueous concentration of adsorbing ions at temperatures above and well below the gel-to-fluid phase transition temperature of DPPC. The electrophoretic mobility data were then analyzed in terms of the Langmuir-Stern-Grahame model (20, 21). The model contains two adsorption parameters that can be derived from experimental results: the association constant and the membrane surface area per adsorbed ion. In this study we show how the packing density and the conformational state of hydrocarbon chains in DPPC membranes affect the adsorption of ions; we also describe how a simple mobile discrete charge model for ions adsorbed in the membrane provides explanation for the areas observed as ion adsorption sites.

MATERIALS AND METHODS

Materials

DPPC was obtained from Avanti Polar Lipids (Birmingham, AL) and PCP, 99% pure, was obtained from Aldrich Chemical Co. (Milwaukee, WI). Other chemicals were at least reagent grade.

Preparation of lipid vesicles

We used multilayered vesicles prepared by manually shaking the suspending aqueous medium in a round bottom flask. The glass surface of the flask had a thin film of DPPC deposited on it; the deposition was accomplished by evaporating the chloroform of a chloroform-DPPC solution in the flask using a Flash-Evaporator by Buchler Instruments (Fort Lee, NJ). The temperature of the suspension medium was ~45°C, i.e., higher than the gel-to-fluid phase transition temperature of DPPC. Unless stated otherwise, the aqueous medium used in the electrophoretic mobility studies contained 0.03 M KCl and a potassium phosphate/citrate/borate buffer (0.002/0.002/0.0005 M) at pH 10. High pH values are necessary to exclude adsorption of neutral PCP. Details are described in reference 21.

Electrophoretic mobility measurements

The electrophoretic mobility of DPPC vesicles was measured using a model Mark-1 instrument with a thermally insulated water tank from Rank Instruments (Bottisham, Cambridge, UK). The measurements were done at 42 and 25°C, corresponding to the fluid and gel states of DPPC, respectively. The electrophoretic mobility was converted into ζ-potential using the Helmholtz equation $\mu = \epsilon\epsilon_0\zeta/\eta$ (22), where ϵ is the dielectric constant of water, $\epsilon_0 = 8.85 \times 10^{-12}$ F/m, and η the viscosity of water at a given temperature. Each experimental data point was obtained from ~20–30 measurements using alternating polarity of the applied field and determining the drift velocity of vesicles as a function of depth of focus of the microscope. The measurements were done in the vicinity of the stationary layer and the drift velocity at the stationary layer was obtained using linear regression.

Analysis of ζ-potential isotherms

ζ-potential is the electrostatic potential difference between the shear surface where the aqueous medium moves with respect to the membrane surface and the bulk aqueous solution. It follows from the numerical integration of Poisson's equation, using the method given in reference 23, that the changes of electric potential over short distances Δx for the ionic content of aqueous medium used in our studies, are satisfactorily approximated by $\exp(-\Delta x/d)$. Using this approximation the ζ-potential can be related to the membrane surface potential V_m according to

$$\zeta = V_m \exp(-s/d), \tag{1}$$

where d is the screening distance of the Debye-Huckel theory (24). The sheer distance, s, was determined from the calibration given in reference 21, $s = 0.255$ nm for the solutions with 0.03 M KCl + buffer, and $s = 0.33$ nm for solutions with 0.002 M KCl + buffer. The membrane surface potential is related to surface charge density σ_m by the condition of electroneutrality, which in MKS-SI units is given by

$$\sigma_m + \{2kT\epsilon\epsilon_0 \Sigma C_{i0} [\exp(-z_i e V_m/kT) - 1]\}^{1/2} = 0. \tag{2}$$

C_{i0} is the volume density of ions of charge $z_i e$ in the bulk aqueous solution and ϵ is the dielectric constant of water.

The surface charge density of DPPC membrane is determined by the surface density of adsorbed organic ions $(A^-)_m$

$$\sigma_m = -e(A^-)_m. \tag{3}$$

The surface density of adsorbed ions $(A^-)_m$ depends on the strength of ion-membrane interactions given by the association constant, K, the concentration of the adsorbing species on the aqueous side of the interface, $[A^-]_m$, and the number of unoccupied sites per unit area. $(A^-)_m$ is obtained from the Langmuir adsorption model according to

$$(A^-)_m = (K/P_s)[A^-]_m/(1 + K[A^-]_m), \tag{4}$$

where P_s is the membrane surface area associated with the adsorption site.

The repulsion of negatively charged adsorbing species from the negatively charged membrane is accounted for by a Boltzmann factor

$$[A^-]_m/[A^-]_0 = \exp(eV_m/kT), \tag{5}$$

where $[A^-]_0$ is the bulk concentration.

The adsorbing ions are distributed between the membranes of the vesicles and water. If $[L]$ is the molar concentration of lipids and $[A^-]_{aq}$ is the total concentration of A^- species in the suspension, then their distribution between membranes and water is accounted for by

$$[A^-]_{aq} = [A^-]_0 + (A^-)_m[L]N_{AV}P_l, \quad (6)$$

where P_l is the area per lipid in the membrane and N_{AV} is Avogadro's number.

The adsorption parameters K and P_s were obtained by χ^2 minimization method based on a gradient expansion algorithm described in reference 25. Their standard deviations were obtained as the square root of the diagonal elements of the error matrix.

Two quantities of interest can be derived from the adsorption parameters K and P_s: (*a*) the linear partition coefficient, β,

$$\beta = K/P_s \quad (7)$$

which relates the surface density of ions, $(A^-)_m$ to their volume density at the aqueous side of the membrane/water interface, $[A^-]_m$. The definition of β follows from the linear portion of the Langmuir adsorption isotherm (Eq. 4). (*b*) The Gibbs free energy change, ΔG^0, is related to the ratio of volume densities of adsorbing species within the membrane adsorption layer $(A^-)_m/\delta$ to that at the aqueous side of the membrane/water interface $[A^-]_m$.

$$\exp(-\Delta G^0/RT) = \beta/\delta, \quad (8)$$

where δ is the width of the membrane adsorption layer. According to arguments given in reference 19 and to make our results comparable with those given in the literature (13, 19) the estimates of ΔG^0 given in this paper are based on $\delta = 0.4$ nm.

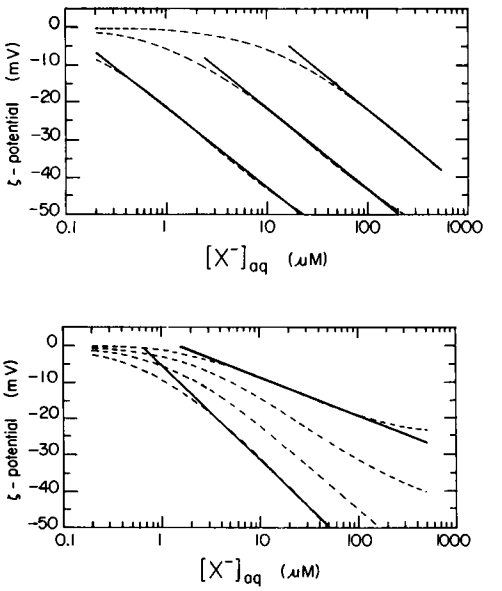

FIGURE 1 Characteristic features of the ζ-potential isotherms due to the adsorption of negatively charged ions X^-. The broken curves show the isotherms computed from the adsorption model. The solid lines illustrate the main feature of the isotherms within the typical range of experimental ζ-potential values. (*a*) Shift of the isotherms due to the change of the association constant K for a fixed value of the area of adsorption sites, P_s: $K = 1.0 \times 10^6$, 1.0×10^5, 1.0×10^4 M^{-1} (*left to right*), $P_s = 3.5$ nm^2. (*b*) Change of the slope of the isotherms due to the change of the area of adsorption sites P_s for a given K: $P_s = 1.4$, 2.8, 5.6, 11.2 nm^2 (*left to right*), $K = 7.5 \times 10^4$ M^{-1}.

RESULTS AND DISCUSSION

ζ-potential isotherms and adsorption characteristics

Adsorption characteristics of PCP^- and of lipophilic ions $TPhB^-$ and DPA^- are characterized by two parameters: the association constant, K, and the membrane surface area of adsorption sites, P_s. In Fig. 1, we illustrate how these two adsorption parameters affect the ζ-potential isotherm. On semilogarithmic plots, the changes in K result in shifts of the isotherms along the concentration axis (Fig. 1 *a*). The variations of P_s, within the intermediate range of concentrations, alter the slope (Fig. 1 *b*) of the ζ-potential isotherms. We have selected realistic ranges of parameters and plotted the theoretical values of the ζ-potential up to -50 mV, which represents a typical upper limit of the magnitude of the experimental ζ-potential.

Although it was not possible to establish reliable saturation levels of ζ-potential isotherms due to solubility problems, the plots shown in Fig. 1 indicate that one can distinguish the changes of the association constant from the changes of the area of adsorption sites on the transition from the gel to the fluid state of the membrane.

ζ-potential isotherms for gel and fluid membranes

Semilogarithmic plots of the dependence of ζ-potential of DPPC vesicles as a function of the aqueous concentration of PCP^- at two different ionic strengths are shown in Fig. 2. The upper sets of data were obtained at 25°C and characterize PCP^- adsorption to the membrane in the gel state whereas the lower data sets were obtained at 42°C and reflect PCP^- adsorption to fluid membranes. In reference to properties of ζ-potential isotherms illustrated in Fig. 1, the major change in the transition from the gel state to the fluid state is the shift of the isotherm along the $[PCP^-]_{aq}$ axis. Because the ζ-potential is the measure of the density of charge on the otherwise neutral membrane, the data indicate much stronger adsorption of PCP^- to the membrane in the fluid state. The solid curves represent the fits of the adsorption model described in Materials and Methods when both sets of data for low and high ionic strength were combined.

The association constant, K, the membrane surface area per adsorption site, P_s, and the linear partition coefficient β of DPPC membranes and PCP^- obtained from the fit of the adsorption model to the ζ-potential

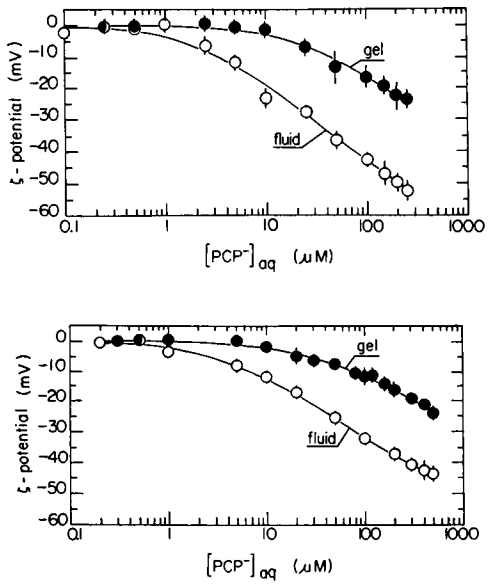

FIGURE 2 ζ-potential isotherms of PCP^- and DPPC membranes. The isotherms for the gel state and the fluid state were obtained at 25 and 42°C, respectively. Conditions: pH 10, phosphate/citrate/borate buffer 0.002/0.002/0.0005 M; (*a*) 0.002 M KCl, (*b*) 0.03 M KCl.

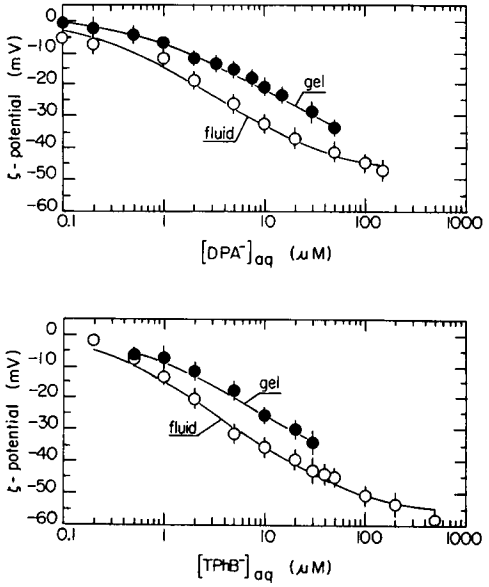

FIGURE 3 ζ-potential isotherms of lipophilic ions and DPPC membranes. The isotherms for the gel state and the fluid state were obtained at 25 and 42°C, respectively. Conditions: pH 10, 0.03 M KCl, phosphate/citrate/borate buffer 0.002/0.002/0.0005 M; (*a*) DPA^-, (*b*) $TPhB^-$.

isotherms are given in Table 1 *a*. .The parameters reflect the one order of magnitude difference between the association constant and the partition coefficient of PCP^- between the gel and fluid membranes.

In Fig. 3 we present the ζ-potential isotherms of lipophilic ions DPA^- and $TPhB^-$. These results were obtained in suspensions containing 0.03 M KCl, i.e., under conditions comparable to those applicable to the PCP results shown in Fig. 2 *b*. With respect to PCP^-, the ζ-potential isotherms for DPA^- and $TPhB^-$ are shifted along the concentration axis toward the lower values indicating higher affinity of the membrane to these ions as compared with PCP^-. This applies to both the gel and fluid state. A notable difference between the PCP^- and other lipophilic ions is the significantly smaller concentration shifts of the isotherms between the gel and fluid states. The adsorption characteristics of the lipophilic ions obtained from the fit of the model (*solid curves*) to the experimental data are summarized in Table 1 *b*.

TABLE 1*a* Adsorption characteristics of PCP^- and DPPC membranes

	Assoc. constant	Ads. site area	Partition coeff.
	K, M^{-1}	P_s, nm^2	β, m
gel	$(4.9 \pm 2.8) \times 10^3$	5.4 ± 2.3	$(1.5 \pm 0.9) \times 10^{-6}$
fluid	$(4.5 \pm 0.9) \times 10^4$	4.5 ± 0.4	$(1.7 \pm 0.3) \times 10^{-5}$

The adsorption site areas obtained from the Langmuir model represent the membrane surface area occupied by one molecule. In most of the past studies of adsorption on lipid bilayer membranes the adsorption sites were not well defined or were not the center of interest. In some cases, such as adsorption of calcium and other inorganic divalent cations, each negatively charged lipid molecule can be regarded as the adsorption site as was concluded from the existence of the reversal of polarity of the ζ-potential (26). The assumptions of 1:1 or 1:2 binding stoichiometries are expected not to be applicable to large molecular ions that intercalate into the bilayer. As a result of adsorption of PCP^-, DPA^-, and $TPhB^-$ one would expect formation of a domain of localized deformation of lipids centered around the intercalated molecular ion. A region defining the area of adsorption site was expected to

TABLE 1*b* Adsorption characteristics of lipophilic ions and DPPC membranes

	Assoc. constant	Ads. site area	Partition coeff.
	K, M^{-1}	P_s, nm^2	β, m
DPA^-			
gel	$(2.5 \pm 1.0) \times 10^5$	5.9 ± 1.2	$(7.1 \pm 0.3) \times 10^{-5}$
fluid	$(7.4 \pm 2.1) \times 10^5$	5.2 ± 0.4	$(2.4 \pm 0.7) \times 10^{-4}$
$TPhB^-$			
gel	$(3.1 \pm 1.0) \times 10^5$	5.0 ± 1.7	$(1.0 \pm 0.7) \times 10^{-4}$
fluid	$(5.9 \pm 1.4) \times 10^5$	4.1 ± 0.2	$(2.4 \pm 0.6) \times 10^{-4}$

depend on the size and shape of the molecular ion as well as on the physical state of membrane lipids. Instead, as the results in Table 1 suggest, it appears that the area of adsorption site is about the same regardless of the molecular structure of adsorbing species, and, individually, there are no significant differences between the site areas in the gel and fluid membranes.

For the purpose of further discussion we will consider the weighted average of 5 nm^2 as the characteristic area of the adsorption site. However, the data in Tables 1*a* and 1*b* taken as a group, hint that the area of adsorption sites in the gel membrane may be greater than the area in the fluid membrane. Further studies should resolve the uncertainty. Altenbach and Seelig (27) addressed the problem of adsorption of positively charged tetraphenylphosphonium ion (TPP^+) to PC membranes by relating the magnitude of quadrupole splitting of the deuterated choline segment of PC to $[TPP^+]_{aq}$ using the Langmuir adsorption model and determining the membrane surface potential from the Gouy-Chapman theory. Their analysis yielded 8.3 lipid molecules per adsorption site which represents an area of ~6 nm^2. It was encouraging to find that for another type of lipophilic ion along with using a method very different from ours the magnitude of the area of the adsorption site was similar to that obtained in the present study. As pointed out by one of the reviewers, the ratio of the number of lipids per adsorption site, P_s/P_{lipid} in the gel state is about double of that in the fluid state. Using P_{lipid} (gel) = 0.46 nm^2 (15) and P_{lipid} (fluid) = 0.71 nm^2 (18), it follows from the values of adsorption site areas given in Tables 1*a* and 1*b*, that the weighted averages of P_s/P_{lipid}, including all the adsorbing species, are 12.1 ± 2.4 for the gel and 6.1 ± 0.2 for the fluid state of DPPC membranes.

Interactions between adsorbed ions in the gel and fluid DPPC membranes

The independence of adsorption site areas on both the ionic size and the conformational state of lipids in the membrane has led us to the assumption that the adsorption site areas may be determined by the electrostatic interactions between ions adsorbed in the membrane. This assumption was supported by the results of earlier studies of adsorption of PCP^- on egg-PC membranes (21) indicating no significant dependence of adsorption parameters on the change of ionic strength from 0.02 to 0.32 M.

In the following section we compare our experimental results with the predictions of a simple discrete charge model. We assume that ions are adsorbed at some depth, *l*, below the membrane-water interface, and laterally diffuse as discrete mobile charges. With each ion we can associate a disk of radius R_c where the potential energy of the repulsive ion-ion interactions exceeds the thermal energy *kT*. The adsorbed ions polarize the aqueous salt solution on both sides of the membrane which decreases their potential energy. We ignore the second interface because the effect of polarization of the far aqueous interface is offset by the repulsive interaction between ions across the membrane. The model of the interface consists of two semi-infinite media: an aqueous salt solution and a lipid monolayer with an infinitely thick hydrocarbon core region. A pair of ions adsorbed at depth *l* below the membrane-water interface and separated by a distance *r* are depicted in Fig. 4.

The polarization of the aqueous medium by the adsorbed ions causes the electric field created by these ions inside the membrane to be noncoulombic. The polarized aqueous solution can be replaced by the membrane-like dielectric and the charges induced at the interface can be replaced by the image charges $q_1' = -\omega q_1$ and $q_2' = -\omega q_2$ (23). For complete electrostatic screening of the adsorbed ions by counterions in the aqueous medium, i.e., regarding the aqueous solution to be a perfect conductor, one can assume $\omega = 1$. Even in the absence of a salt solution, $\omega = (\epsilon_{aq} - \epsilon_m)/(\epsilon_{aq} + \epsilon_m)$. The screening distance of the aqueous solution in our studies was ~1 nm and thus the screening of adsorbed ions by counterions is appreciable over the distances of our interest. Because the polarization of the water solution and the screening by counter-ions are additive, it will be assumed that ω is equal to unity.

It follows from the diagram in Fig. 4 that the potential energy of charges q_1 and q_2, adsorbed at a depth *l* within the membrane boundary region of dielectric constant ϵ_m,

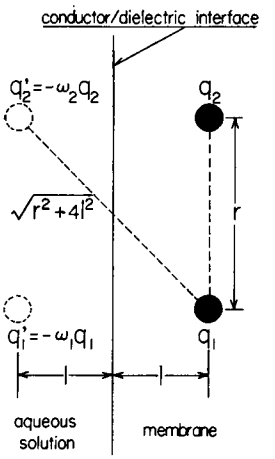

FIGURE 4 Model of membrane/water interface illustrating two ions q_1 and q_2 separated by a distance *r* and adsorbed at a depth *l* below the level of penetration of water in the membrane. Due to the presence of aqueous solution, the interaction between ions adsorbed in the membrane is noncoulombic. The polarization of the interface is accounted for by image charges q_1' and q_2'.

is equal to

$$U(r, l, \epsilon_m) = q_1[V_2(r) - V_2(\infty)]$$
$$= (q_1 q_2/4\pi\epsilon\epsilon_m)[1/r - \omega/\sqrt{(r^2 + 4l^2)}]. \quad (9)$$

The dependence of potential energy between two adsorbed ions of equal charge on the ion-ion separation, r, and the adsorption depth, l, is shown in Fig. 5. For shallow adsorption (case U_1) the close proximity of the aqueous solution significantly reduces the repulsive interactions between the adsorbed ions as compared with ions adsorbed deeper in the membrane (case U_2). Due to thermal motion the ions can approach each other up to a distance R_c corresponding to $U/kT = 1$. For deep adsorption, R_c is greater than for shallow adsorption; in terms of adsorption to the membrane this results in a lower packing density of adsorbed ions and a lower surface coverage for a given aqueous concentration and a given association constant. Following the ideas used in various versions of discrete charge models (10, 28–30) we associate with each of the adsorbed ion an area P_s

$$P_s = \pi R_c^2 \quad (10)$$

and identify P_s as the area of the adsorption site. The exclusion radius R_c follows from

$$U(R_c, l, \epsilon_m) = kT. \quad (11)$$

The dielectric constant ϵ_m signifies the average dielectric constant within the membrane boundary region.

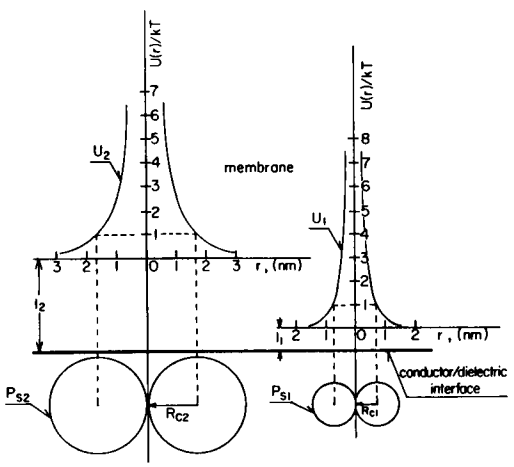

FIGURE 5 Illustrates the dependence of electrostatic potential energy on the separation of ion pairs adsorbed at various depths below the membrane-water interface and the concept of a cut-off disk model. The potential energy U computed according to Eq. 7 for $\epsilon_m = 10$ was normalized to thermal energy at 300 K. For shallow adsorption we assumed an adsorption depth of $l_1 = 0.2$ nm (case U_1) and for deep adsorption (case U_2) $l_2 = 0.8$ nm.

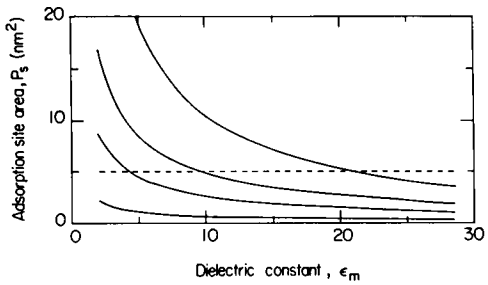

FIGURE 6 Dependence of adsorption site area on the dielectric constant of the interfacial region for various depth of ion adsorption. Adsorption depth l = 1.0, 0.5, 0.3, 0.1 nm (*top down*), T = 300 K. The broken horizontal line indicates the representative experimental value of the adsorption site area of 5 nm².

Fig. 6 shows how the adsorption site area depends on the dielectric constant for several values of adsorption depth. The broken horizontal lines at 5 nm² indicate the representative value of the adsorption site area determined from the experimental results.

The potential energy of ion-ion repulsion is determined both by ϵ_m and l. Because we do not know how ϵ_m is related to l, we plot in Fig. 7 the relationship between ϵ_m and l for constant adsorption sites areas (4, 5, and 6 nm²) according to the above model. For the typical experimental value of adsorption site area of 5 nm², the model predicts a range of paired values for the dielectric constant and the adsorption depth. At the low end, the value of P_s = 5 nm² would correspond to an adsorption depth of ~0.2 nm and the dielectric constant of 2. At the high end, for an adsorption depth of 1 nm the corresponding dielectric constant would have to be ~20. Both limiting values are unrealistic in view of the polarity profile of the membrane which is trapezoidal rather than rectangular (31). For deeply adsorbed ions one would prefer to use a low

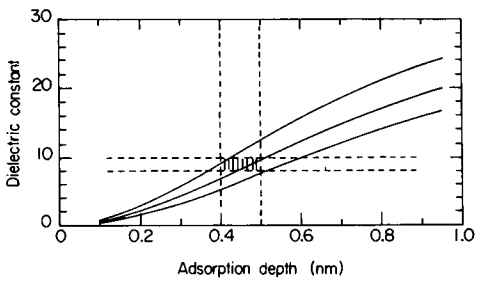

FIGURE 7 Relationship between the dielectric constant of the membrane boundary region and the adsorption depth for a given adsorption site area. The solid curves represent (*top-down*) P_s = 4.0, 5.0, and 6.0 nm². The experimental values of P_s fall within the area delimited by a dielectric constant of 8–10 and an adsorption depth of 0.4–0.5 nm.

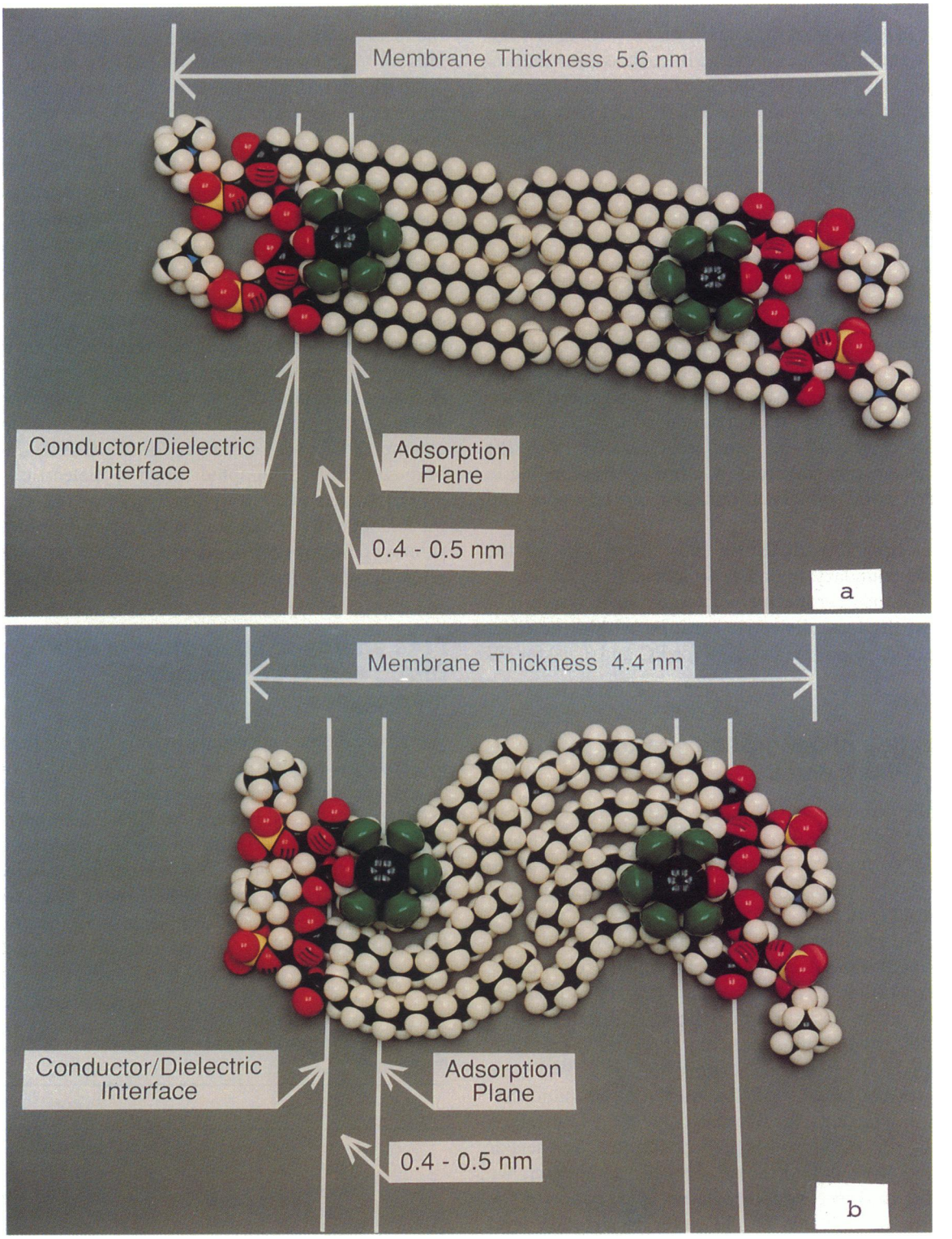

FIGURE 8 Molecular model depicting location of PCP^- in DPPC membranes in the gel (*a*) and the fluid state (*b*).

dielectric constant of ~3 because the adsorbed ion is primarily in the hydrocarbon environment with only a few solvated water molecules present. In contrast, for shallow adsorption, above the region of glycerol backbone of phospholipids and within the polar head groups the dielectric constant is expected to be significantly greater, ~30.

We have shown by the horizontal dotted lines in Fig. 7 the range of dielectric constants of special significance. Constants between 8 and 10 were obtained for PCP^- adsorbed in egg-PC membranes from the analysis of the shifts of UV absorption spectra of ionized PCP by means of Onsager-like models (8). For $P_s = 5$ nm^2 curve the vertical dotted lines delimit the adsorption depth of 0.4–0.5 nm. Although the experimental values of the adsorption site areas have not been determined accurately, the ranges of the dielectric constant, 8–10, and the adsorption depth, 0.4–0.5 nm, are consistent with the range of adsorption site areas, 4–6 nm^2, corresponding to our experimental values as indicated by the upper and lower curves.

The selection of a dielectric constant of ~10 for the membrane boundary region is supportable by other results. For optical probe merocyanine-540 it was established that the local dielectric constant within the chromophore adsorption region is 6–8 for PC and 8–10 for PS (32).

Localization of adsorption site of PCP^-, $TPhB^-$, and DPA^-

The mobile discrete charge model assumes the existence of a sharp interface between the conductive aqueous medium and the membrane. The question arises as to where to locate this interface since the adsorption depth l is referenced to it.

There are numerous characteristic planes defined for the lipid membranes whose position is highly relevant for the interpretation of the x-ray and neutron diffraction data (33). A consensus has been developed to locate the hydrophobic/hydrophilic boundary close to the first CH_2 group of the hydrocarbon chains (34, 35). We have assumed various locations of the interface and found that there is a satisfactory overall consistency if the interface is placed at the carbonyl oxygen group of the deeper penetrating hydrocarbon chain. By this assignment we are identifying the conductor/dielectric interface of the model with the location of the water penetration level proposed earlier by Simon and McIntosh (34). This results in placing the charge centers of PCP^-, $TPhB^-$, and DPA^- at the level of the third and fourth carbons of the hydrocarbon chains. The location of PCP^- within the DPPC membrane in the gel and fluid state is shown in Fig. 8 using the molecular models.

There are several results in the literature identifying the location and properties of the adsorption of lipophilic ions in membranes. In a theoretical study (13), the optimum parameters used in the dipolar model, which predicts satisfactorily the change in Gibbs free energy on adsorption of $TPhB^-$ and TPP^+ (Table 2 in reference 13), are a dielectric constant of 10 and the location of the adsorption layer 2 nm from the center of membrane, i.e., also below the region of carbonyl oxygens. In another study, the decrease of the transmembrane translocation rate constant of DPA^- with the increase of its aqueous concentration was explained in terms of a discrete charge model of the interface (10) similar to ours. The increase of the translocation rate constant resulted in an empirical relationship between the depth of adsorption and the dielectric constant of the membrane boundary region. These were $l(\text{nm}) = 0.025\ \epsilon_m$ for the dioleylphosphatidylcholine and $l(\text{nm}) = 0.06\ \epsilon_m$ for the GMO/Chol membranes. Using our adopted range of dielectric constants 8–10, the predicted adsorption depths are 0.2–0.25 nm for the former and 0.5–0.6 nm for the latter membranes. Our values of adsorption depth 0.4–0.5 nm fall within the range derived from their empirical relationships.

Free energy of adsorption of PCP^-, DPA^-, and $TPhB^-$ on DPPC membranes

We have assumed according to reference 19 the width of the adsorption layer to be 0.4 nm and determined the Gibbs free energy changes associated with the adsorption of PCP^-, DPA^-, and $TPhB^-$ to DPPC membranes in the gel and fluid states (Table 2). There are several notable features of these results. The free energy changes for the adsorption of DPA^- and $TPhB^-$ are the same within the experimental errors. This applies both to the gel and the fluid states. The differences between ΔG° values, $\Delta\Delta G^\circ = \Delta G^\circ$ (gel) $- \Delta G^\circ$ (fluid) for DPA^- and $TPhB^-$ are about

TABLE 2 Gibbs free energy of ion adsorption to DPPC membranes

	ΔG^0
	kcal/mol
PCP^-	
gel	−4.9 ± 0.4
fluid	−6.7 ± 0.1
DPA^-	
gel	−7.2 ± 0.25
fluid	−8.3 ± 0.18
$TPhB^-$	
gel	−7.4 ± 0.4
fluid	−8.3 ± 0.15

the same (~1 kcal/mol or 43 meV/ion) despite the very different shapes of these molecular ions. In contrast, for PCP^- we found a much greater difference, 1.8 kcal/mol (78 meV/ion). PCP^- is a smaller molecule than DPA^- or $TPhB^-$, and resembling a disk. Therefore it is possible that the entropy change on adsorption of PCP to a membrane in the gel state is smaller than that in the fluid state. The behavior of PCP and other small biologically active molecules in lipid matrix as a function of conformational order of membrane lipids is an interesting problem in view of the lipid matrix-mediated mechanism of biological activity (36). Better insight into the thermodynamics of binding of PCP to lipid bilayers can be obtained from the measurements of the temperature dependence of the adsorption parameters for the gel and fluid membranes.

This work was supported by grants from the Medical Research Foundation of Oregon and the National Institutes of Health (1RO1 ES 5202). This paper is the Environmental Sciences and Resources Program Publication No. 254.

Received for publication 2 May 1990 and in final form 17 July 1990.

REFERENCES

1. Weinbach, E. C. 1956. Biochemical basis for the toxicity of pentachlorophenol. *Science (Wash. DC)*. 124:940.
2. Weinbach, E. C., and J. Garbus. 1965. The interaction of uncoupling phenols with mitochondria and mitochondrial protein. *J. Biol. Chem.* 240:1811–1819.
3. Maher, P., and S. J. Singer. 1984. Structural changes in membranes produced by the binding of small amphipathic molecules. *Biochemistry*. 23:232–240.
4. Smejtek, P., A. W. Barstad, and S. Wang. 1989. Pentachlorophenol-induced change of zeta-potential and gel-to-fluid transition temperature in model lecithin membranes. *Chem. Biol. Interact.* 71:37–61.
5. Smejtek, P., K. Hsu, and W. H. Perman. 1976. Electrical conductivity of lipid bilayer membranes induced by pentachlorophenol. *Biophys. J.* 16:319–336.
6. McLaughlin, S. G. A., and J. P. Dilger. 1980. Transport of protons across membranes by weak acids. *Physiol. Rev.* 60:825–863.
7. Jayaweera, R., R. Petersen, and P. Smejtek, 1982. Induced hydrogen ion transport in lipid membranes as origin of toxic effect of pentachlorophenol in an alga. *Pestic. Biochem. Physiol.* 18:197–204.
8. Smejtek, P., A. W. Barstad, and K. Hsu. 1987. Dielectric properties of adsorption/ionization site of pentachlorophenol in lipid membranes. *Biochim. Biophys. Acta*. 902:109–127.
9. Andersen, O. S., S. Feldberg, H. Nakadomari, S. Levy, and S. McLaughlin. 1978. Electrostatic interactions among hydrophobic ions in lipid bilayer membranes. *Biophys. J.* 21:35–67.
10. Wang, C. C., and L. J. Bruner. 1978. Evidence for a discrete charge effect within lipid bilayer membranes. *Biophys. J.* 24:749–764.
11. Smejtek, P., and M. Paulis-Illangasekare. 1979. Modification of ion transport in lipid bilayer membranes in the presence of 2,4-dichlorophenoxyacetic acid. II. Suppression of tetraphenylborate conductance and changes of interfacial potentials. *Biophys. J.* 26:467–488.
12. Ellena, J. F., R. N. Dominey, S. J. Archer, Z. C. Xu, and D. S. Cafiso. 1987. Localization of hydrophobic ions in phospholipid bilayers using ^1H nuclear overhauser effect spectroscopy. *Biochemistry*. 26:4584–4592.
13. Flewelling, R. F., and W. L. Hubbell. 1986. The membrane dipole potential in a total membrane potential model. Applications to hydrophobic ion interactions with membranes. *Biophys. J.* 49:541–552.
14. Gennis, R. B. 1989. Biomembranes: Molecular Structure and Function. Springer-Verlag, New York. 235–269.
15. Wiener, M. C., R. M. Suter, and J. F. Nagle. 1989. Structure of the fully hydrated gel phase of dipalmitoylphosphatidylcholine. *Biophys. J.* 55:315–325.
16. Small, D. M. 1986. The Physical Chemistry of Lipids. Plenum Press, New York. 629 pp.
17. Seelig, J., and A. Seelig. 1980. Lipid conformation in model membranes and biological membranes. *Q. Rev. Biophys.* 13:19–61.
18. Lis, L. J., M. McAlister, N. Fuller, R. P. Rand, and V. A. Parsegian. 1982. Interactions between neutral phospholipid bilayer membranes. *Biophys. J.* 37:657–666.
19. Flewelling, R. F., and W. L. Hubbell. 1986. Hydrophobic ion interactions with membranes. Thermodynamic analysis of tetraphenylphosphonium binding to vesicles. *Biophys. J.* 49:531–540.
20. McLaughlin, S., and H. Harary. 1976. The hydrophobic adsorption of charged molecules to bilayer membranes: a test of the applicability of the Stern equation. *Biochemistry*. 15:1941–1948.
21. Smejtek, P., S. Wang, and A. W. Barstad. 1987. Adsorption of ionized and neutral pentachlorophenol to phosphatidylcholine membranes. *Biochem. Biophys. Acta*. 905:213–221.
22. Aveyard, R., and D. A. Haydon. 1973. An Introduction to the Principles of Surface Chemistry. Cambridge University Press, London. 52–57.
23. Bentz, J., and S. Nir. 1980. Cation binding to membranes: competition between mono-, di- and trivalent cations. *Bull. Math. Biol.* 42:191–220.
24. Brown, R. H. 1974. Membrane surface charge: discrete and uniform modelling. *In* Progress in Biophysics and Molecular Biology. J. A. V. Butler and D. Noble, editors. Pergamon Press, New York. 28:343–370.
25. Bevington, P. R. 1969. Data Deduction and Error Analysis for the Physical Sciences. McGraw-Hill, New York. 235–245.
26. McLaughlin, S., N. Mulrine, T. Gresalfi, G. Vaio, and A. McLaughlin. 1981. Adsorption of divalent cations to bilayer membranes containing phosphatidylserine. *J. Gen. Physiol.* 77:445–473.
27. Altenbach, C., and J. Seelig. 1985. Binding of the lipophilic cation tetraphenylphosphonium to phosphatidylcholine membranes. *Biochim. Biophys. Acta*. 818:410–415.
28. Tsien, R. Y. 1978. A virial expansion for discrete charges buried in a membrane. *Biophys. J.* 24:561–567.
29. Tsien, R. Y., and S. B. Hladky. 1982. Ion repulsion within membranes. *Biophys. J.* 39:49–56.

30. McLaughlin, S. 1989. The electrostatic properties of membranes. *Annu. Rev. Biophys. Biophys. Chem.* 18:113–136.

31. Griffith, O. H., P. J. Dehlinger, and S. P. Van. 1974. Shape of the hydrophobic barrier of phospholipid bilayers (Evidence for water penetration in biological membranes). *J. Membr. Biol.* 15:159–192.

32. Lelkes, P. I., and I. R. Miller. 1980. Perturbations of membrane structure of optical probes: I. Location and structural sensitivity of merocyanine 540 bound to phospholipid membranes. *J. Membr. Biol.* 52:1–15.

33. Scherer, J. R. 1989. On the position of the hydrophobic/hydrophilic boundary in lipid bilayers. *Biophys. J.* 55:957–964.

34. Simon, S. A., and T. J. McIntosh. 1986. Depth of water penetration into lipid bilayers. *In* Methods in Enzymology. L. Packer, editor. Academic Press Inc, New York. 127:511–521.

35. Herbette, L. G., D. W. Chester, and D. G. Rhodes. 1986. Structural analysis of drug molecules in biological membranes. *Biophys. J.* 49:91–94.

36. Rhodes, D. G., J. G. Samiento, and L. G. Herbette. 1985. Kinetics of binding of membrane active drugs to receptor sides. Diffusion limited rates for a membrane bilayer approach of 1,4-dihydropyridine calcium channel antagonists to their active site. *Mol. Pharmacol.* 27:612–623.